

Doubly ranked tests for grouped functional data

Mark J. Meyer

Department of Mathematics and Statistics, Georgetown University
Washington, DC USA

Abstract

Nonparametric tests for functional data are a challenging class of tests to work with because of the potentially high dimensional nature of functional data. One of the main challenges for considering rank-based tests, like the Mann-Whitney or Wilcoxon Rank Sum tests (MWW), is that the unit of observation is a curve. Thus any rank-based test must consider ways of ranking curves. While several procedures, including depth-based methods, have recently been used to create scores for rank-based tests, these scores are not constructed under the null and often introduce additional, uncontrolled for variability. We therefore reconsider the problem of rank-based tests for functional data and develop an alternative approach that incorporates the null hypothesis throughout. Our approach first ranks realizations from the curves at each time point, then summarizes the ranks for each subject using a sufficient statistic we derive, and finally re-ranks the sufficient statistics in a procedure we refer to as a doubly ranked test. As we demonstrate, doubly rank tests are more powerful while maintaining ideal type I error in the two sample, MWW setting. We also extend our framework to more than two samples, developing a Kruskal-Wallis test for functional data which exhibits good test characteristics as well. Finally, we illustrate the use of doubly ranked tests in functional data contexts from material science, climatology, and public health policy.

1 Introduction

Expanded research in functional data analysis has produced a variety of tests couched in the framework of classic nonparametric tests including work by [Hall and Van Keilegom \[2007\]](#), [López-Pintado and Romo \[2009\]](#), [López-Pintado et al. \[2010\]](#), [Chakraborty and Chaudhuri \[2015\]](#), [Pomann et al. \[2016\]](#), [López-Pintado and Wrobel \[2017\]](#), [Abramowicz et al. \[2018\]](#), [Berrett et al. \[2021\]](#) and [Meléndez et al. \[2021\]](#). These various authors have built out hypothesis testing procedures for functional versions of Mann-Whitney or Wilcoxon Rank Sum, Anderson-Darling tests, and permutation tests, among others. The primary feature of functional data that makes the development of such nonparametric tests challenging is that the unit of observation is a curve. For example, $X_{g,1}(s), \dots, X_{g,n_g}(s)$ are a sample of n_g curves from groups $g = 1, \dots, G$. Each curve is typically measured on a fine grid, $\mathcal{S} = \{s : s = s_1, \dots, s_S\}$ for a total of S measurements. Any rank-based procedure must employ a way to rank curves directly or at least rank summary metrics of each subject's curve.

Depth is a popular and useful concept for ranking functions and many authors have utilized depth for Mann-Whitney-Wilcoxon (MWW) type tests [[López-Pintado and Romo, 2009](#), [López-Pintado et al., 2010](#), [López-Pintado and Wrobel, 2017](#)], functional boxplots [[Sun and Genton,](#)

2011, Genton et al., 2014, Wrobel et al., 2016], outlier detection [Sun and Genton, 2012, Dai and Genton, 2018, Huang and Sun, 2019, Dai et al., 2020, Alemán-Gómez et al., 2022], and ranking curves [López-Pintado and Romo, 2009, 2011, Sun et al., 2012, Sguera and López-Pintado, 2021]. The basic idea behind depth is to characterize the proportion of time a curve is bounded above and below by another curve in the sample. The resulting scores, when ordered, rank the curves from the inside out with the smallest values representing the extremes, the maximum or minimum, and the largest value representing the median [López-Pintado and Romo, 2009, Sun et al., 2012]. These scores are effectively a measure of the distance a curve is from the middle. MWW-type tests using depth to test for a difference between two groups must construct a third, artificial reference group [López-Pintado and Romo, 2009, López-Pintado et al., 2010, López-Pintado and Wrobel, 2017]. Depth is first determined by group, then the test procedure counts the number of depth values in each group that are larger than the depth in the reference group. Code is publicly available for the depth-based MWW test, see López-Pintado and Wrobel [2017].

Alternative approaches include a spatial sign-based statistic by Chakraborty and Chaudhuri [2015] and a random projections based approach by Meléndez et al. [2021]. In the former, Chakraborty and Chaudhuri [2015] develop an MWW-type statistic using the spatial sign for infinite-dimensional data that weakly converges to a Gaussian distribution under limited assumptions. The spatial sign is used as a distance metric to construct the test, taking pairwise distances between groups with data assumed to arise from a random variable defined on a separable Hilbert space. The latter alternative approach, a random projection-based test by Meléndez et al. [2021], maps the points from the high dimensional functional space to a randomly chosen low-dimensional space defined using Brownian motion. This approach has application in parametric tests for grouped functional as well, see for example Cuesta-Albertos and Febrero-Bande [2010]. The random projections-based approach effectively generates scores for each subject via a random basis function and an integral approximation of the subject-specific curve. It then treats these scores as the data in a traditional MWW test, thus the scores are ranked and then summed by group. Neither of these alternative methods have publicly available code.

Both depth- and random projection-based approaches perform well in larger samples [López-Pintado and Romo, 2009, López-Pintado et al., 2010, Meléndez et al., 2021]. However, each method also introduces an additional and uncontrolled for source of variation: the random artificial reference group for the depth-based approach and the brownian motion-based basis functions for the random projections. While depth is useful for ranking curves particularly when identifying medians and outliers, it does not produce a score that ranks in a traditional fashion, from smallest to largest. When using random projections, the integration is performed before constructing ranks which ignores the fact that rank may be dynamic over time. To handle the curve ranking problem, both procedures rely on subject-specific summary scores, although neither constructs their scores under the null. Thus, the tests are only conducted under the null when comparing the scores between groups.

The spatial sign-based approach differs from the depth- and random projection-based methods in that, for finite-dimensional approximations of functional data, it effectively creates a time-point specific score instead of subject-specific scores over time. Chakraborty and Chaudhuri [2015] show that the spatial sign-based test performs well empirically when the underlying data is Gaussian with a relatively small sample. The test does consider the MWW null

throughout its construction, but appears to be underpowered when the data is non-Gaussian. While all of these methods are formulated for the MWW or two group case, to our knowledge no prior work considers the Kruskal-Wallis (KW) or three or more group case. Thus, with respect to these authors, we believe that a further examination of this problem is warranted.

In this manuscript, we re-examine rank-based test settings for comparing groups of functional data. We propose a general testing procedure working within the MWW or KW assumptions, developing our tests under the relevant null hypotheses at all stages—a general overview of MWW and KW tests as well as functional data is given in Section 2. Our approach first constructs ranks of either the raw data or preprocessed functional data at each discretely measured time point giving every subject a curve of ranks. Under the MWW and KW null hypotheses, we then derive the exact and approximate distribution of each subject’s r th order statistic at a given time point (Section 3). The resulting approximate distribution can be shown to be an exponential family member from which we obtain sufficient statistics for each subject’s value of r . The summaries resulting from the sufficient statistic become our new data, or rank-based scores, which are then ranked and analyzed in the usual way by the relevant tests. Because the MWW and KW tests ultimately re-rank our rank-based scores, we refer to our testing procedures as doubly ranked tests.

We empirically demonstrate the power of doubly ranked tests in Section 4. Our approach can accommodate curves with a potentially large number of measurements and groups of size $G \geq 2$. Further, we show that doubly ranked tests perform well in both small and larger sample sizes. We illustrate their use with an analysis of data from several different studies across different substantive fields (Section 5). The illustrations include data on resin viscosity, Canadian weather patterns, and changes in driving requests in the United States prior to and just after the initiation of COVID-19 policy measures in various states. While we formulate doubly ranked tests in the functional data context with the preprocessed data using functional principal components, the tests are applicable to any high dimensional data testing setting. We discuss this, and our work in general, in Section 6.

2 Statistical Framework

Because our method blends several statistical frameworks, we now briefly describe each beginning with the MWW and KW tests in their scalar forms. We then discuss some general concepts for functional data. Functional data analysis is a large area of research. Review articles by Morris [2015], Wang et al. [2016], and Greven and Scheipl [2017], for example, or the text by Ramsay and Silverman [2005] will provide more in-depth discussions of this topic.

2.1 Mann-Whitney-Wilcoxon

Let X_1, \dots, X_{n_1} be observed data from group 1, Y_1, \dots, Y_{n_2} be observed data from group 2, and $n = n_1 + n_2$. Assuming the groups are independent, the null and alternative hypotheses can have one of two forms. The first tests for stochastic ordering where the null is $H_0 : F_X(c) = F_Y(c)$ and the alternative is $H_A : F_X(c) \leq F_Y(c)$ for the CDFs $F_X(c)$ and $F_Y(c)$ in each group. Assuming these distributions are same up to location shift Δ , i.e. $F_X(c) =$

$F_Y(c - \Delta)$, gives a second form of the hypotheses which is $H_0 : \Delta = 0$ and $H_A : \Delta \neq 0$.

The test statistic to test either form of H_0 is $T^+ = T - \frac{n_2(n_2+1)}{2}$ where $T = \sum_{i=1}^{n_2} R[Y_i]$ for $R[Y_i]$ equal to the rank of Y_i among the combined samples, i.e. among $X_1, \dots, X_{n_1}, Y_1, \dots, Y_{n_2}$. The sum of the ranks, T , is the test statistic for the Wilcoxon rank sum test [Wilcoxon, 1945, Kloeke and McKean, 2015]. T^+ is also equivalent to the test statistic described by Mann and Whitney [1947]. Consequently, we refer to this test as the MWW test.

The exact distribution of T is non-standard but can be easily computed by standard statistical software for samples up to $n = 50$, provided there are no tied ranks. For larger samples and in the presence of ties, a normal approximation to the distribution of the ranks is used instead, see the `wilcox.test()` documentation in the `stats` package in R [R Core Team, 2022]. The test statistic based off of the normal approximation is

$$T_z = \left[T - \frac{n_2(n+1)}{2} \right] / \sqrt{\frac{n_1 n_2 (n+1)}{12}},$$

which has a standard normal distribution.

2.2 Kruskal-Wallis

The KW test generalizes the MWW to three or more groups [Kruskal and Wallis, 1952, Kloeke and McKean, 2015]. Let G denote the total number of independent groups with data $X_{g,1}, \dots, X_{g,n_g}$ for $g = 1, \dots, G$. The KW test assumes the distributions of the data are the same except possibly for some location parameter or parameter(s). The null hypothesis for the KW test generalizes the second MWW null where groups differ only up to some set of location shifts, Δ_g . The null then has the form $H_0 : \Delta_1 = \dots = \Delta_G$ with the alternative hypothesis, $H_A : \Delta_g \neq \Delta_{g'}$ for some $g \neq g'$.

For $n = \sum_{g=1}^G n_g$, the test statistic to test H_0 is

$$H = \frac{12}{n(n+1)} \sum_{g=1}^G n_g \left(\bar{R}_g - \frac{n+1}{2} \right)^2,$$

where \bar{R}_g is the average rank in group g , i.e. $\bar{R}_g = n_g^{-1} \sum_{i=1}^{n_g} R[X_{g,i}]$. Under H_0 , H is distribution-free. Tables for its exact distribution do exist, see for example Hollander and Wolfe [1999], Chapter 6. H is asymptotically χ_{G-1}^2 under H_0 as well, see Kruskal and Wallis [1952] or Kloeke and McKean [2015] which is what the `stats` package in R uses when `kruskal.test()` is called [R Core Team, 2022].

2.3 Functional Data

Functional data are data observations whose units are curves, often measured over time but they can be measured over location as well. These curves are typically sampled at a high frequency over a pre-defined interval. The data comes sampled on a grid, $\{s : s = s_1, \dots, s_S\}$ for example as we note in Section 1. The data used for analysis may be the raw values themselves, $X_1(s), \dots, X_{n_1}(s)$, or they may be preprocessed and projected into a

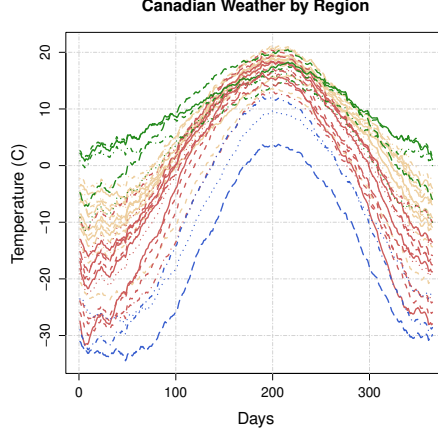


Figure 1: Blue curves denote the stations in the Arctic region, tan curves indicate stations the Atlantic region, red curves for stations in the Continental region, and green curves are the Pacific region.

well-behaved space using a known basis function. The idea behind preprocessing is to model the underlying function from which the raw data values were observed and then analyze the functions themselves. We denote the preprocessed data with $\tilde{X}_1(s), \dots, \tilde{X}_{n_1}(s)$. There are many ways to preprocess functional data including functional principal components, wavelet-based techniques, and Fourier transforms [Wang et al., 2016]. Our method is compatible with either raw or pre-processed data, but for this work we will preprocess functional data using a sandwich smoother-based approach referred to as Fast Covariance Estimation or FACE [Xiao et al., 2013, 2016]. FACE is a nonparametric approach for constructing functional principal components based on a set of curves with a potentially large sampling density. It can be implemented using the `refund` package in R [Goldsmith et al., 2022]. As an example, Figure 1 contains the preprocessed (using FACE) daily temperature curves from the Canadian Weather dataset [Ramsay and Silverman, 2005, Ramsay et al., 2009]. The dataset contains daily temperature and precipitation measurements, averaged over the years 1960 to 1994 from 35 different sites across Canada. We analyze this data in Section 5.

3 Doubly Ranked Tests

Suppose we obtain a sample of curves from two or more groups: $X_{g,1}(s), \dots, X_{g,n_g}(s)$ for $g = 1, \dots, G$, $s = s_1, \dots, s_S$, and $n_1 + \dots + n_g + \dots + n_G = n$. Measurements are discretely sampled on the same grid, $\mathcal{S} = \{s : s = s_1, \dots, s_S\}$, and come from continuous process. Under the null, we assume no difference in the curves between the G groups across all s . To avoid having to make a distributional assumption on the process that generates $X_{g,i}(s)$, we evaluate this null by analyzing the ranks of $X_{g,i}(s)$ at each measurement occurrence s , i.e. time point or location depending on what the function is measured over. Thus, we first rank either the raw or preprocessed data at each measurement occurrence, ignoring group assignment. This results in a curve of ranks for each subject which we denote as $z_{g,i}(s)$. If there is no difference in the curves across s under the null, then we should also observe no difference in the ranks

across s . Assuming each subject's curve has a true order in the sample, we can consider $\{z_{g,i}(s_1), \dots, z_{g,i}(s_S)\}$ as a set of draws from the distribution describing that true order. We then construct a summary of each curve and re-rank the summaries for analysis using either the MWW or KW tests, depending on the number of groups. Assuming the summaries are reasonable representations of the subject's order in the sample, no difference in the curves and subsequent ranks over s between the groups implies no difference in the summarized ranks between the groups.

More formally, the doubly ranked test inherits the null and alternatives from the MWW and KW tests. Since the summaries are based on a sample of observed ranks, it is reasonable to assume the distributions are the same up to some location shift. Let $t_1, t_2, \dots, t_g, \dots, t_G$ denote the observed summarized ranks from their corresponding random variables $T_1, T_2, \dots, T_g, \dots, T_G$. The doubly ranked MWW test then has the null and alternative of $H_0 : \theta = 0$ and $H_0 : \theta \neq 0$ where θ is a parameter such that $F_{T_1}(t_1) = F_{T_2}(t_2 - \theta)$. When $G \geq 3$, the null and alternative hypotheses for the doubly ranked KW test are $H_0 : \theta_1 = \dots = \theta_G$ with the alternative hypothesis, $H_A : \theta_g \neq \theta_{g'}$ for some $g \neq g'$. In other words, under H_0 we assume there is no difference between the groups in the location parameters of the distributions of summarized ranks. The alternative is that there is a difference, when $G = 2$, and at least one difference, when $G \geq 3$.

3.1 Test Derivation

As in the univariate tests, the ranks are randomly assigned under H_0 . We apply this both at the measurement occurrence level and again at the summary level when the summaries are re-ranked. Thus, for each subject and at each measurement occurrence, $z_{g,i}(s) \sim \mathcal{U}\{1, n\}$ where n is the total number of curves and \mathcal{U} denotes the discrete uniform distribution. To obtain the summaries, consider the sampling distribution of the r th order statistic for any given subject at time s which we denote $Z_{(r)}$. We let z generically denote an observed rank, i.e. $z_{g,i}(s)$, for ease of derivation. The PMF for $Z_{(r)}$ is given by

$$P\left[Z_{(r)} = z\right] = 1 - \sum_{k=0}^{r-1} \binom{n}{k} \left(\frac{z}{n}\right)^k \left(1 - \frac{z}{n}\right)^{n-k} - \left[1 - \sum_{k=0}^{r-1} \binom{n}{k} \left(\frac{z-1}{n}\right)^k \left(1 - \frac{z-1}{n}\right)^{n-k}\right]. \quad (1)$$

The summations in Equation (1) are the CDFs of binomial random variables with probabilities of success $\frac{z}{n}$ and $\frac{z-1}{n}$, respectively. Let $I_q(a, b)$ denote the regularized incomplete beta function evaluated at q with parameters a and b . Equation (1) can be re-expressed as

$$P\left[Z_{(r)} = z\right] = I_{z/n}(r, n - r + 1) - I_{(z-1)/n}(r, n - r + 1). \quad (2)$$

The distribution in Equation (2) is non-standard and difficult to work with analytically, although we can compute values from it using standard statistical software. The relationship

between the beta and binomial distributions can, however, be exploited to find an approximation of $P[Z_{(r)} = z]$ with a more workable form. Specifically, the regularized incomplete beta functions in Equation (2) are also equivalent to the CDFs of beta random variables evaluated at $\frac{z}{n}$ and $\frac{z-1}{n}$, respectively, with parameters r and $n - r + 1$. After expressing the beta CDFs in their integral form, we re-write $P[Z_{(r)} = z]$ as

$$\begin{aligned} P[Z_{(r)} = z] &= \frac{\Gamma(n+1)}{\Gamma(r)\Gamma(n-r+1)} \left[\int_{\frac{z}{n}-\frac{1}{n}}^{\frac{z}{n}} t^{r-1} (1-t)^{n-r} dt \right]. \end{aligned}$$

A full derivation of $P[Z_{(r)} = z]$ is in Appendix A.

We approximate the integral using the midpoint rule and select one interval, $[\frac{z}{n} - \frac{1}{n}, \frac{z}{n}]$, with a midpoint at $\frac{z}{n} - \frac{1}{2n}$. This value is also approximately equal to the optimal numerical solution to the mean value theorem problem for this integral, see Section 1 of Supplement A [Meyer, 2024a] for a numerical comparison. The mass function in (2) can then be approximated by

$$\begin{aligned} P[Z_{(r)} = z] &\approx \frac{\Gamma(n+1)}{\Gamma(r)\Gamma(n-r+1)} \frac{1}{n} \\ &\times \left(\frac{z}{n} - \frac{1}{2n} \right)^{r-1} \left(1 - \frac{z}{n} + \frac{1}{2n} \right)^{n-r}, \end{aligned} \quad (3)$$

with the approximation improving as n increases. We observe this graphically in Section 1 of Supplement A [Meyer, 2024a]. When $r = \frac{n+1}{2}$, the expected rank under H_0 , the approximation is quite good.

Claim 1. *The distribution described by the mass function in Equation 3 is an exponential family member.*

Proof. The proof of Claim 1 is in Appendix B. □

Since Equation (3) is an exponential family, $t(z) = \log \left[\left(\frac{z}{n} - \frac{1}{2n} \right) / \left(1 - \frac{z}{n} + \frac{1}{2n} \right) \right]$ is a sufficient statistic for r . Noting that, under H_0 , $z \sim \mathcal{U}\{1, n\}$, the statistic has a useful property when applied to the sample of ranks.

Claim 2. *Under H_0 , $E[t(z)] = 0$.*

Proof. The proof of Claim 2 is in Appendix C. □

It is straightforward to show that $t(z) = 0$ only when $z = \frac{n+1}{2}$, which is the expected value of a discrete uniform distribution on the interval $\{1, n\}$. Thus, the sufficient statistic preserves this property in its expectation under the null. In the context of the sample of ranks for subject i in group g , r is the true order of subject i 's curve within the sample,

under H_0 . Subsequently, we summarize each $z_{g,i}(s)$ over s using the sufficient statistic

$$t[z_{g,i}(\mathcal{S})] = \frac{1}{S} \sum_{s=1}^S \log \left[\frac{\frac{z_{g,i}(s)}{n} - \frac{1}{2n}}{1 - \frac{z_{g,i}(s)}{n} + \frac{1}{2n}} \right]. \quad (4)$$

Our testing procedure for grouped functional data proceeds as follows: 1) preprocess the data using FACE; 2) generate ranks at each time point s ignoring group assignment; 3) calculate $t[z_{g,i}(\mathcal{S})]$; 4) perform the relevant test (MWW or KW), depending on G . The doubly ranked MWW test statistic is

$$T_{DR}^+ = \sum_{j=1}^{n_2} R(t[z_{2,i}(\mathcal{S})]) - \frac{n_2(n_2 + 1)}{2}.$$

For $G \geq 3$, the doubly ranked KW test statistic is

$$H_{DR} = \frac{12}{n(n+1)} \sum_{g=1}^G n_g \left[\overline{R(t[z_{g,i}(\mathcal{S})])} - \frac{n+1}{2} \right]^2,$$

where $\overline{R(t[z_{g,i}(\mathcal{S})])} = \frac{1}{n_g} \sum_{i=1}^{n_g} R(t[z_{g,i}(\mathcal{S})])$. Because the sufficient statistic is a one-to-one transformation of the ranks, when $S = 1$, the doubly ranked tests will be equivalent to their univariate analogue, i.e. the standard MWW or KW test. The statistic $t[z_{g,i}(\mathcal{S})]$ is a univariate score for each subject which use as the “new” data in each backend test. Thus, the distributional results from Section 2 hold for both the doubly ranked MWW and KW tests. That is, T_{DR}^+ is approximately normal while H_{DR} is asymptotically χ_{G-1}^2 . Implementation of our method is available for download as an R package, titled `runDRT`, at <https://github.com/markjmeyer/runDRT>.

4 Simulation Study

In our empirical study, we assume a balanced design with groups of size $n_1 = n_2 = 10, 25$ and 50 and, in the KW case, n_3 defined similarly. The total sample sizes are $n = 20, 50$, and 100 (MWW) and $n = 30, 75$, and 150 (KW). The doubly ranked MWW test is for two groups and we consider the three group case for the doubly ranked KW test. To simulate the functional data, we use the approach employed by Chakraborty and Chaudhuri [2015] who generate data in the MWW setting using a Karhunen-Loève expansion of the form

$$X_{1,i}(s) = \sum_{k=1}^K \sqrt{2}[(k-0.5)\pi]^{-1} Z_{ik} \sin[(k-0.5)\pi s],$$

for those in group X . The value Z_{ik} is a random variable which we generate from one of three distributions: Gaussian, t_2 (a t distribution with 2 degrees of freedom), and log-normal. Formally, the value of K could be infinite. In simulation, we take it to be large, $K = 1000$

basis functions. To generate the data in the other group(s), we use:

$$X_{g,j}(s) = \mu(s) + \sum_{k=1}^K \sqrt{2} [(k - 0.5)\pi]^{-1} Z_{jk} \sin [(k - 0.5)\pi s],$$

where $\mu(s)$ is a time-dependent function for $s \in [0, 1]$, $g = 2$ for the MWW case, and $g = 2, 3$ for the KW setting. These generative models produce functional data with high levels of autocorrelation, see Section 2 of Supplement A [Meyer, 2024a].

We consider three different functional forms for $\mu(s)$:

$$\begin{aligned} \mu_1(s) &= \xi s, \mu_2(s) = \xi 4s(1 - s), \text{ and} \\ \mu_3(s) &= \xi m^{-1} B(2, 6)^{-1} s^{2-1} (1 - s)^{6-1}, \end{aligned}$$

for m equal to $\max_s B(2, 6)^{-1} s^{2-1} (1 - s)^{6-1}$ and $B(2, 6)$ equal to the Beta function evaluated at 2 and 6. The parameter ξ is set to zero to evaluate Type I Error and incremented up to 3, by steps of size 0.12, to evaluate power. The length of the sampling grid, s , varies from sparser to denser: $S = 40, 80, 160$, and 320 and is taken to be equally spaced over the unit interval. We limit our direct comparison to the depth-based method, since it alone has publicly available code. All curves are preprocessed using FACE, retaining 99% of the variability. Code to generate the empirical studies is in Supplement B [Meyer, 2024b].

Type I error estimates for the both the doubly ranked MWW test and the depth-based test are presented in Table 1 while Table 2 contains type I error for the doubly ranked KW test. Because type I error did not vary significantly by S , both tables contain values under the sparsest sampling density ($S = 40$) and are broken down by distribution of Z_k and total sample size, n . Each empirical type I error rate is based on 10000 simulated datasets. Testing was performed at the $\alpha = 0.05$ level. The doubly ranked MWW test achieves or is within Monte Carlo error of the nominal α -level for the larger sample sizes ($n = 50, 100$), regardless of the distribution of Z_k (Table 1). Under smaller sample sizes, the empirical type I error rate is below nominal, near 0.041 for each Z_k (Table 1). Type I error is more stable in the doubly ranked KW test simulation with all but one setting either achieving nominal or within Monte Carlo error of it; when $Z_k \sim t_2$, the error is under nominal, 0.046 (Table 2). Notably, from Table 1, the error rates are similar between doubly ranked and depth-based MWW tests with depth-based test error rates tending to be under nominal for $n = 20$ (0.031 to 0.032) and nearing or achieving nominal as n increases. Additional results for type I error under other sampling densities ($S = 80, 160$ and 320) are in Section 2 of Supplement A [Meyer, 2024a].

Power curves are based on 5000 simulated datasets for each combination of ξ , S , n , $\mu(s)$, and distribution of Z_k . Figure 2 presents the curves under the sparsest sampling density ($S = 40$) since increasing the sampling density does not significantly impact the power of the doubly ranked MWW test. Solid curves denote the settings where $n = 100$, dashed were $n = 50$, and dotted-dashed for when $n = 20$. Curves for the doubly ranked MWW test are in blue while curves for the depth-based MWW test are in tan. The rows of Figure 2 index the distribution of Z_k and the columns index the varying functional forms of $\mu(s)$. Overall, power increases for both methods as n increases, no matter the distribution of Z_k and the form of

Table 1: Type I Error for functional Mann-Whitney-Wilcoxon tests by distribution of Z_k and sample size when $S = 40$ and 320 . Each value is based on 10000 simulated datasets. G stands for Gaussian, T for t_2 , and L for log-normal.

S	Z_k	n	Doubly Ranked	Depth-based
40	G	20	0.042	0.031
		50	0.052	0.041
		100	0.050	0.049
	T	20	0.042	0.032
		50	0.048	0.044
		100	0.047	0.050
	L	20	0.041	0.032
		50	0.051	0.042
		100	0.052	0.049
320	G	20	0.041	0.031
		50	0.052	0.041
		100	0.049	0.049
	T	20	0.041	0.031
		50	0.048	0.045
		100	0.049	0.051
	L	20	0.042	0.033
		50	0.050	0.045
		100	0.050	0.048

Table 2: Type I Error for doubly ranked Kruskal-Wallis tests by distribution of Z_k and sample size when $S = 40$ and 320 . Each value is based on 10000 simulated datasets. G stands for Gaussian, T for t_2 , and L for log-normal.

S	n	Z_k		
		G	T	L
40	30	0.051	0.046	0.050
	75	0.049	0.050	0.049
	150	0.051	0.048	0.051
320	30	0.052	0.046	0.049
	75	0.048	0.051	0.049
	150	0.051	0.048	0.051

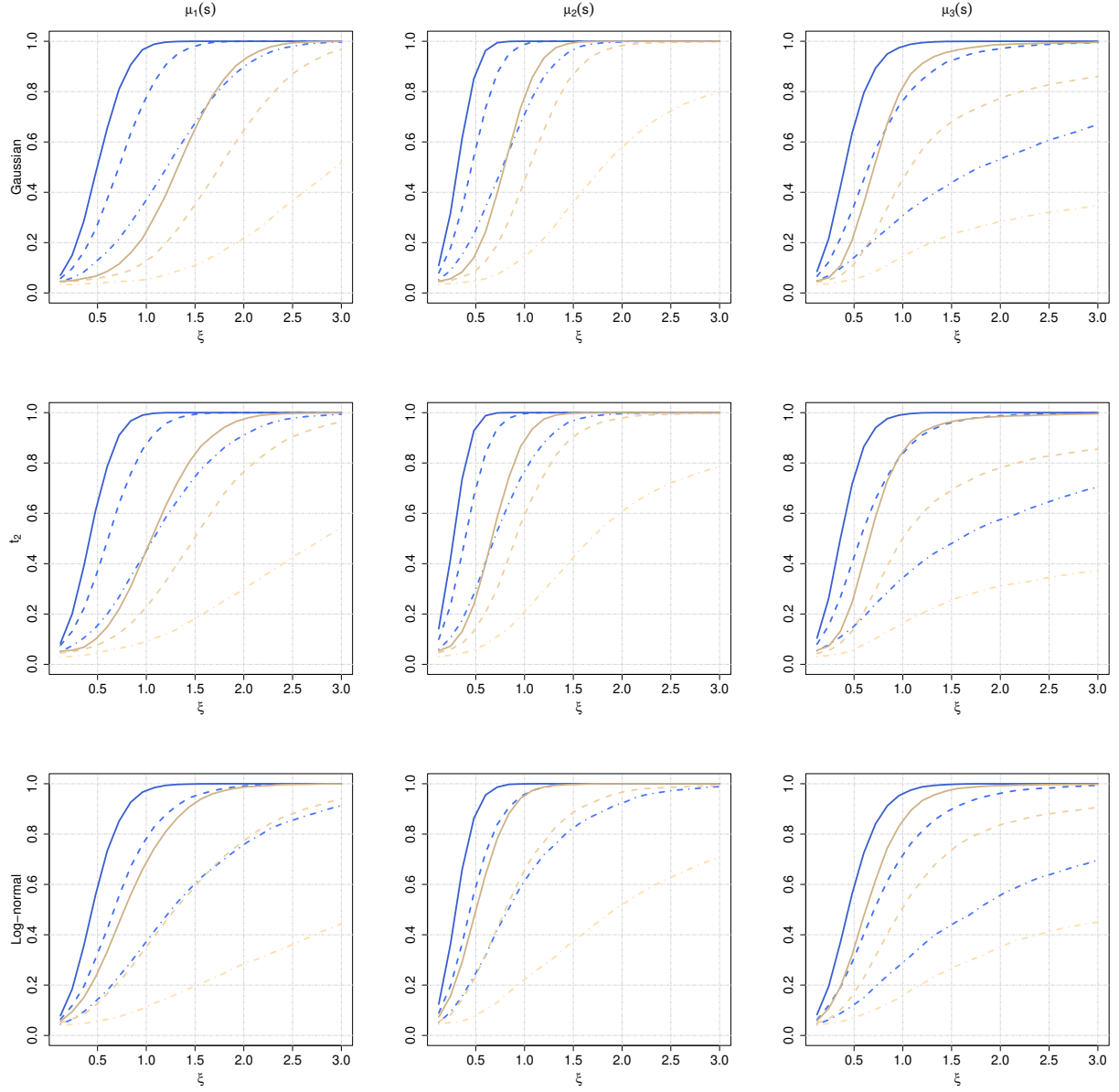


Figure 2: Power curves for functional Mann-Whitney-Wilcoxon tests under the sparsest sampling density, $S = 40$. Rows index varying distributions of Z_k , columns index values of $\mu(s)$. Curves for the doubly ranked test are in shades of blue, curves for depth-based tests are in shades of tan. Solid curves are for when $n = 100$, dashed curves for when $n = 50$, and dotted-dashed curves for when $n = 20$.

Table 3: Test statistics and p -values for doubly ranked tests applied to the three data illustrations: resin viscosity, Canadian weather, and COVID mobility. Temp. is short for temperature, Cur. for curing, Rot. for rotational, and Precip. for precipitation. Doubly ranked KW tests were performed for both Canadian weather outcomes and the COVID mobility factor MD, VA, & WV. The remaining tests were doubly ranked MWW tests.

Data Set	Outcome	Factor	Test Statistic	p -value
Resin	Viscosity	Resin Temp.	194	< 0.001
		Cur. Agent Temp.	440	0.337
		Tool Temp.	207	< 0.001
		Rot. Speed	419.5	0.217
		Mass Flow	507.5	0.957
Weather	Temp.	Region	21.44	< 0.001
	Precip.	Region	22.46	< 0.001
COVID	Requests	CO & UT	132	0.001
		IA & MN	1871	< 0.001
		MD, VA, & WV	2.214	0.331

$\mu(s)$. Comparing the two and at a given n , the doubly ranked MWW test has consistently higher power than the depth-based MWW test. Similar power curves to those in Figure 2 when $S = 80, 160$ or 320 are in Section 2 of Supplement A [Meyer, 2024a].

Figure 3 contains the power curves for the doubly ranked KW test when $S = 40$. As with the MWW tests, the curves are based on 5000 simulated datasets per combination of ξ , n , $\mu(s)$, and distribution of Z_k . Solid curves now denote the settings where $n = 150$, dashed where $n = 75$, and dotted-dashed for when $n = 30$. Overall, power increases as n increases across Z_k and forms of $\mu(s)$. The form of $\mu(s)$ does have a slight impact on power when n is small but the distribution of Z_k does not appear to have much of an impact on power. Additional power curves when $S = 80, 160$, and 320 are in Section 3 of Supplement A [Meyer, 2024a].

5 Data Illustrations

To illustrate both doubly ranked MWW and KW tests, we examine functional data from three different substantive fields with varying numbers of observations and differing lengths of functions. Two of the datasets are available in R packages and the third will be made available upon request. Each dataset has at least one factor of interest that may differentiate the outcome curves. While we will draw light conclusions based on the findings, the purpose of these illustrations is to demonstrate the use of doubly ranked tests and not to elaborate on the scientific findings (or lack thereof) that result from our analysis. Results from all three data sources for various combinations of outcomes and factors are in Table 3. All outcomes were first pre-processed using FACE, retaining 99% of the variation within the curves. Graphs of the functional curves from each data source are in Section 4 of Supplement A [Meyer, 2024a].

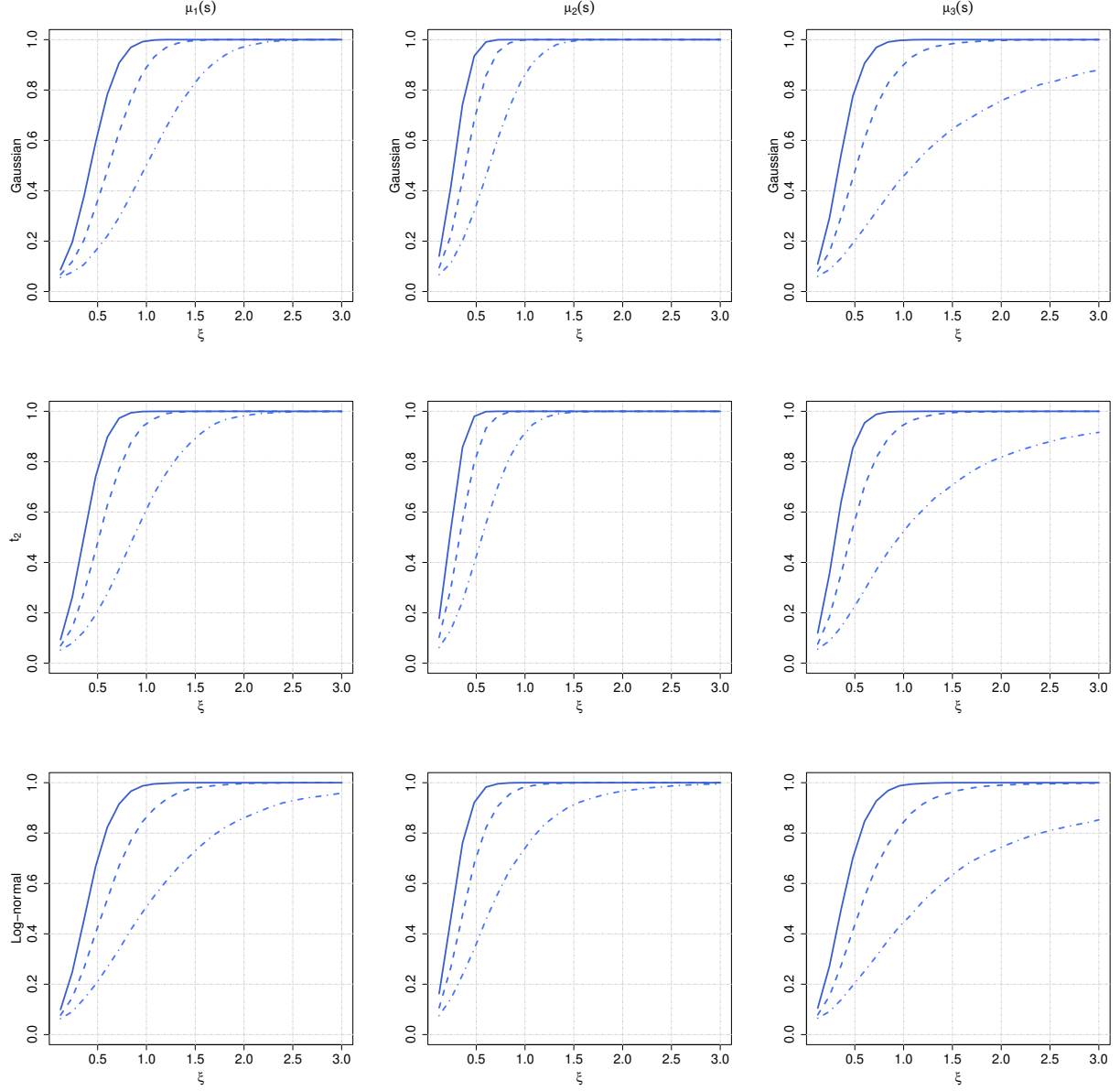


Figure 3: Power curves for doubly ranked Kruskal-Wallis tests under the sparsest sampling density, $S = 40$. Rows index varying distributions of Z_k , columns index values of $\mu(s)$. Solid curves are for when $n = 100$, dashed curves for when $n = 50$, and dotted-dashed curves for when $n = 20$.

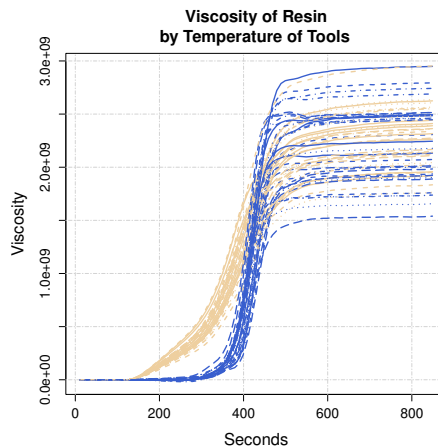


Figure 4: Blue curves were measured under the “low” temperature condition while tan curves were measured under the “high” temperature condition.

5.1 Resin Viscosity

The resin viscosity data comes from an experimental setting conducted at the Technical University of Munich’s Institute for Carbon Composites and is freely available in the R package `FDBoost` [Brockhaus et al., 2020]. The data set contains measurements of the viscosity of resin over the course of 838 seconds with the goal assessing factors that influence the curing process in a resin mold. The grid is not equally spaced due to technical reasons whereby viscosity can be measured every two seconds at first but, due to hardening, can only be measured every ten seconds after the 129th second. In total, 64 different molds were poured under five different experimental conditions: temperature of resin, temperature of the curing agent, temperature of the tools, rotational speed, and mass flow. Each condition is a binary factor, with a “low” and “high” levels.

From Table 3, we observe that in two of five factors the location parameters in the distributions of the ranks differ significantly. Specifically, the resin temperature ($W = 194$, $p = < 0.001$) and tool temperature ($W = 207$, $p < 0.001$) have p -values below nominal. This suggests that the ranks of the curves that describe the viscosity of the resin differ significantly between the groups defined by these factors. To determine which group is higher or lower, we turn to a graphical assessment. When considering the tool temperature, Figure 4 displays clear clustering in the curves with low temperature tools appearing to induce slower curing than high temperature tools. This separation lessens around 400 seconds where the sets of curves begin to overlap. The analysis by temperature of resin captures greater separation after 400 seconds which can be seen in the additional figures in Section 4 of Supplement A [Meyer, 2024a]. The remaining factors did not significantly distinguish the curves as can also be seen in the graphs in Section 4 of Supplement A [Meyer, 2024a].

5.2 Canadian Weather

The Canadian weather data is a classic dataset for illustrating functional data analysis techniques having appeared in texts by Ramsay and Silverman [2005] and Ramsay et al. [2009]

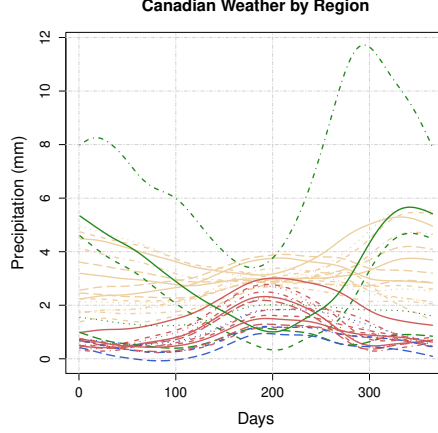


Figure 5: Blue curves denote the stations in the Arctic region, tan curves indicate stations the Atlantic region, red curves for stations in the Continental region, and green curves are the Pacific region.

as well as in many articles that are too numerous to list here. It contains daily average temperature (C) and precipitation (mm) measurements, averaged over the years 1960 to 1994, taken at 35 different sites across Canada. The factor of interest is the region from which the measurement was taken: Arctic, Atlantic, Continental, or Pacific. It is available in the R package `fda` [Ramsay et al., 2022]. For the purpose of this illustration, the goal of the analysis is to see if the doubly ranked KW test can detect differences in temperature and precipitation curves by region as might be expected given their geographic differences.

Table 3 contains the results of the analysis for both outcomes. We see that the doubly ranked KW returns significant tests at the nominal level for both temperature curves ($X^2 = 21.44$, $p = < 0.001$) and precipitation curves ($X^2 = 22.46$, $p < 0.001$) differing by region. Formally, we would say the location parameters of the distributions of the summarized ranks for temperature and precipitation over time differ by region. To observe the nature of the difference by group, we examine Figures 1 and 5. We see that the temperature curves from the Arctic region are the coldest while those from the Pacific region tend to be warmest. The precipitation curves show inverted patterns based on region with the Pacific region tending to see more precipitation during the winter months while the Continental and Arctic regions experience more during the summer months.

5.3 COVID Mobility

The COVID mobility data was extracted from publicly available data provided by Apple Inc. regarding daily mapping requests for driving, walking, and transit directions during the onset of the COVID-19 pandemic and for some time thereafter. A cached version of the data is available from Gassen [2022]. The data itself represents the percent change in requests for directions from a baseline date of January 13, 2020. Requests are categorized by whether they were for driving, walking, or transit directions. In our analysis, we focus on the percent change in daily requests for driving directions. For the United States, the data is available at the county level which is our unit of observation.

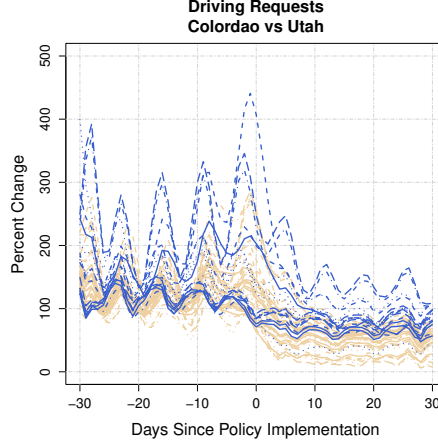


Figure 6: Blue curves denote counties in Utah while tan curves denote counties in Colorado.

Rather than aligning the data by calendar time, we align it by the first date of a major COVID policy implementation at the state level, e.g. shelter-in-place or safer-at-home orders. Policy dates were obtained from the publicly available COVID AMP data [Katz et al., 2023]. The timeline is centered at the date of the first COVID-policy implementation in each state and we take 30 days prior and 30 days post. The main objective of this analysis is to compare different states in similar regions to each other, focusing on whether or not there is a difference post-policy implementation. Specifically, we compare county level percent changes in driving requests between counties in Iowa (IA) and Minnesota (MN), Colorado (CO) and Utah (UT), and finally between Maryland (MD), Virginia (VA), and West Virginia (WV).

When comparing the percent change in county-level requests for driving directions between Colorado and Utah, we find a significant difference between the groups of curves by state ($W = 132$, $p = 0.001$). Figure 6 shows that the county-level curves have substantial overlap pre-initial policy implementation. After implementation, however, Colorado counties tend to experience a lower percent change in requests. Graphs for the remaining comparisons are in Section 4 of Supplement A [Meyer, 2024a]. We see a similar trend when comparing Minnesota and Iowa with Minnesota counties tending to experience lower percent change in driving requests which continues until three to four weeks post-implementation. This is reflected in the doubly ranked MWW test which suggests a significant difference in the location parameters of distributions of the summarized ranks between Minnesota and Iowa ($W = 1871$, $p < 0.001$). In contrast to the first two comparisons, we lack evidence to suggest a difference in the location parameters of the distributions the ranks between Maryland, Virginia, and West Virginia ($X^2 = 2.214$, $p = 0.331$).

6 Discussion

In this manuscript, we investigate two novel nonparametric tests for comparing groups of functional curves: the doubly ranked MWW test and the doubly ranked KW test. The tests arise from the same sufficient statistic derived using the distribution of the ranks under H_0 over time. Treating the ranks from individual curves as a sample over time and using

the sufficient statistic to summarize them allows us to reduce the dimensionality of the testing problem and improve efficiency. While other approaches reduce dimensionality using a summary score for the data, only ours uses a score that is constructed under H_0 . Doubly ranked tests are distribution free since they rely only on the ranks of the sufficient statistics derived in Equation 4. We demonstrate empirically that both the doubly ranked MWW and KW tests perform well in terms of type I error and power for a variety of true error distributions under varying curve types.

The test procedures we propose here are global tests of differences between curves, as are the other methods by [Hall and Van Keilegom \[2007\]](#), [López-Pintado and Romo \[2009\]](#), [López-Pintado et al. \[2010\]](#), [Chakraborty and Chaudhuri \[2015\]](#) and [Meléndez et al. \[2021\]](#). With any global test, one must be careful to examine the underlying data for where the differences lie. These tests can instruct us that there is difference but cannot be used to identify exactly where the difference is nor can they tell us the magnitude of difference. For that, we would need to model the group location curves themselves and rely on point-wise testing, ideally adjusted for multiple testing. See, for example, some of the work on functional regression reviewed in [Morris \[2015\]](#) and [Greven and Scheipl \[2017\]](#).

Point-wise testing is not goal of this work, however our method can be useful as a global test in a variety of data contexts. In our data illustrations, we demonstrate the use of the doubly ranked MWW and KW tests to study problems in material science, climatology, and public health policy. These tests can be performed as a main analysis or a first pass analysis in conjunction with other modeling steps. Our tests are also easy to implement and easy for practitioners to interpret—in particular, for those who are already familiar with univariate MWW and KW tests. Doubly ranked testing is not limited to functional data applications nor is it even limited to FACE-based preprocessed data. The assumptions for the tests apply broadly to both functional and multivariate data.

Our method assumes the sampling grid is the same for each subject. Subjects may, however, have mistimed measurements and therefore asynchronous grids. A full investigation of this data structure is left to future work. However, in the current context, an FPCA that accounts for asynchronous grids can be employed should such data arise. For example, the FPCA by smoothed covariance, see [Yao et al. \[2005\]](#) or [Di et al. \[2009\]](#) among others, can be used in the context of sparse longitudinal data of which asynchronous functional data is a more general case. Such an approach could be used for asynchronously sampled profiles.

A Derivation of the PMF

The full derivation of the exact distribution in Equations (1) and (2) begins with the discrete PMF:

$$\begin{aligned}
 P\left[Z_{(r)} = z\right] &= \sum_{k=r}^n \binom{n}{k} \left[\left(\frac{z}{n}\right)^k \left(1 - \frac{z}{n}\right)^{n-k} \right. \\
 &\quad \left. - \left(\frac{z-1}{n}\right)^k \left(1 - \frac{z-1}{n}\right)^{n-k} \right] \\
 &= \sum_{k=r}^n \binom{n}{k} \left(\frac{z}{n}\right)^k \left(1 - \frac{z}{n}\right)^{n-k} \\
 &\quad - \sum_{k=r}^n \binom{n}{k} \left(\frac{z-1}{n}\right)^k \left(1 - \frac{z-1}{n}\right)^{n-k},
 \end{aligned}$$

from which we obtain Equation (1). To get to Equation (2), we note that the summations in Equation (1) are equivalent to the CDF of the binomial distribution and can be rewritten as regularized incomplete beta functions:

$$\begin{aligned}
 P\left[Z_{(r)} = z\right] &= 1 - I_{1-z/n}[n - (r - 1), r - 1 + 1] \\
 &\quad - \left[1 - I_{1-(z-1)/n}[n - (r - 1), r - 1 + 1]\right],
 \end{aligned}$$

where $I_q(a, b)$ is as defined in Section 3. Regularized incomplete beta functions have the property that $I_q(a, b) = 1 - I_{1-q}(b, a)$. After applying this, we arrive at Equation (2). To obtain the approximate PMF in Equation (3), we note that the CDF of the beta distribution is also a regularized incomplete beta function giving the expression

$$\begin{aligned}
 P\left[Z_{(r)} = z\right] &= \int_0^{\frac{z}{n}} \frac{1}{B(r, n - r + 1)} (t)^{r-1} (1 - t)^{n-r+1-1} dt \\
 &\quad - \int_0^{\frac{z-1}{n}} \frac{1}{B(r, n - r + 1)} (t)^{r-1} (1 - t)^{n-r+1-1} dt \\
 &= \frac{1}{B(r, n - r + 1)} \left[\int_0^{\frac{z}{n}} t^{r-1} (1 - t)^{n-r+1-1} dt \right. \\
 &\quad \left. - \int_0^{\frac{z-1}{n}} t^{r-1} (1 - t)^{n-r+1-1} dt \right].
 \end{aligned}$$

Writing the beta function in terms of gamma functions and combining the integrals, we arrive at Equation (3).

B Proof of Claim 1

Proof. Consider the mass function in Equation (3) and rewrite it as

$$\begin{aligned}
P\left[Z_{(r)} = z\right] &\approx \frac{\Gamma(n+1)}{\Gamma(r)\Gamma(n-r+1)} \frac{1}{n} \\
&\times \left(\frac{z}{n} - \frac{1}{2n}\right)^{r-1} \left(1 - \frac{z}{n} + \frac{1}{2n}\right)^{n-r} \\
&= \frac{\Gamma(n+1)}{\Gamma(r)\Gamma(n-r+1)} \frac{1}{n} \\
&\times \exp\left[n \log\left(1 - \frac{z}{n} + \frac{1}{2n}\right) - \log\left(\frac{z}{n} - \frac{1}{2n}\right)\right] \\
&\times \exp\left[r \log\left\{\left(\frac{z}{n} - \frac{1}{2n}\right) / \left(1 - \frac{z}{n} + \frac{1}{2n}\right)\right\}\right]
\end{aligned}$$

Noting that n is fixed, define the following functions:

$$\begin{aligned}
c(r) &= \frac{1}{n} \frac{\Gamma(n+1)}{\Gamma(r)\Gamma(n-r+1)}, \quad w(r) = r, \\
h(z) &= \exp\left[n \log\left(1 - \frac{z}{n} + \frac{1}{2n}\right) - \log\left(\frac{z}{n} - \frac{1}{2n}\right)\right], \\
&\text{and} \\
t(z) &= \log\left\{\left(\frac{z}{n} - \frac{1}{2n}\right) / \left(1 - \frac{z}{n} + \frac{1}{2n}\right)\right\}.
\end{aligned}$$

The mass function can then be written as

$$P\left[Z_{(r)} = z\right] = h(z)c(r) \exp[w(r)t(z)],$$

which is the form of an exponential family. □

C Proof of Claim 2

Proof. First note the mass function of a discrete uniform random variable over $\{1, n\}$ is $P(Z = z) = \frac{1}{n} \forall z \in \{1, n\}, n \in \mathbb{Z}^+$. The expectation of $t(z)$ is

$$\begin{aligned} E[t(z)] &= E \left[\log \left\{ \left(\frac{z}{n} - \frac{1}{2n} \right) / \left(1 - \frac{z}{n} + \frac{1}{2n} \right) \right\} \right] \\ &= \sum_{z=1}^n \log \left\{ \left(\frac{z}{n} - \frac{1}{2n} \right) / \left(1 - \frac{z}{n} + \frac{1}{2n} \right) \right\} \frac{1}{n} \\ &= \frac{1}{n} \log \left\{ \prod_{z=1}^n \left(\frac{z}{n} - \frac{1}{2n} \right) / \left(1 - \frac{z}{n} + \frac{1}{2n} \right) \right\} \end{aligned}$$

Expanding out the first few terms and last few terms of the product, we see that it is a telescoping product:

$$\begin{aligned} &\prod_{z=1}^n \left(\frac{z}{n} - \frac{1}{2n} \right) / \left(1 - \frac{z}{n} + \frac{1}{2n} \right) = \\ &\quad \frac{\frac{1}{n} - \frac{1}{2n}}{1 - \frac{1}{n} + \frac{1}{2n}} \times \frac{\frac{2}{n} - \frac{1}{2n}}{1 - \frac{2}{n} + \frac{1}{2n}} \times \frac{\frac{3}{n} - \frac{1}{2n}}{1 - \frac{3}{n} + \frac{1}{2n}} \times \dots \\ &\quad \dots \times \frac{\frac{n-2}{n} - \frac{1}{2n}}{1 - \frac{n-2}{n} + \frac{1}{2n}} \times \frac{\frac{n-1}{n} - \frac{1}{2n}}{1 - \frac{n-1}{n} + \frac{1}{2n}} \times \frac{\frac{n}{n} - \frac{1}{2n}}{1 - \frac{n}{n} + \frac{1}{2n}} \\ &= \frac{\frac{1}{2n}}{1 - \frac{1}{2n}} \times \frac{\frac{1}{n} + \frac{1}{n} - \frac{1}{2n}}{1 - \frac{1}{n} - \frac{1}{n} + \frac{1}{2n}} \times \frac{\frac{1}{n} + \frac{2}{n} - \frac{1}{2n}}{1 - \frac{1}{n} - \frac{2}{n} + \frac{1}{2n}} \times \dots \\ &\quad \dots \times \frac{1 - \frac{2}{n} - \frac{1}{2n}}{1 - 1 + \frac{2}{n} + \frac{1}{2n}} \times \frac{1 - \frac{1}{n} - \frac{1}{2n}}{\frac{1}{n} + \frac{1}{2n}} \times \frac{1 - \frac{1}{2n}}{\frac{1}{2n}} \\ &= \frac{\frac{1}{2n}}{1 - \frac{1}{2n}} \times \frac{\frac{1}{n} + \frac{1}{2n}}{1 - \frac{1}{n} - \frac{1}{2n}} \times \frac{\frac{1}{n} + \frac{2}{n} - \frac{1}{2n}}{1 - \frac{2}{n} - \frac{1}{2n}} \times \dots \\ &\quad \dots \times \frac{1 - \frac{2}{n} - \frac{1}{2n}}{\frac{1}{n} + \frac{2}{n} - \frac{1}{2n}} \times \frac{1 - \frac{1}{n} - \frac{1}{2n}}{\frac{1}{n} + \frac{1}{2n}} \times \frac{1 - \frac{1}{2n}}{\frac{1}{2n}} \end{aligned}$$

Examining the last two lines, we see that the first fraction is the reciprocal of the last fraction, the second fraction is the reciprocal of the second to last fraction, the third fraction is the reciprocal of the third to last fraction, and so forth. When n is even, the first $\frac{n}{2}$ fractions will cancel with the last $\frac{n}{2}$ fractions.

When n is odd, the first $\lfloor \frac{n}{2} - 1 \rfloor$ fractions will cancel with the last $\lfloor \frac{n}{2} - 1 \rfloor$ fractions. The remaining fraction will be the $z = \frac{n+1}{2}$ case which equals 1. Thus, for any $n \in \mathbb{Z}^+$, the

product will equal 1. Substituting, we have

$$\begin{aligned} E[t(z)] &= \frac{1}{n} \log \left\{ \prod_{z=1}^n \left(\frac{z}{n} - \frac{1}{2n} \right) \middle/ \left(1 - \frac{z}{n} + \frac{1}{2n} \right) \right\} \\ &= \frac{1}{n} \log(1) = 0 \end{aligned}$$

Thus, the expected value of the sufficient statistic is zero. \square

References

- K. Abramowicz, C. K. Häger, A. Pini, L. Schelin, S. Sjöstedt de Luna, and S. Vantini. Nonparametric inference for functional-on-scalar linear models applied to knee kinematic hop data after injury of the anterior cruciate ligament. *Scandinavian Journal of Statistics*, 45:1036–1061, 2018. doi: 10.1111/sjos.12333.
- Y. Alemán-Gómez, A. Arribas-Gil, M. Desco, A. Elías, and J. Romo. Depthgram: Visualizing outliers in high-dimensional functional data with application to fmri data exploration. *Statistics in Medicine*, 41:2005–2024, 2022. doi: <https://doi.org/10.1002/sim.9342>.
- T. B. Berrett, I. Kontoyiannis, and R. J. Samworth. Optimal rates for independence testing via U-statistic permutation tests. *The Annals of Statistics*, 49:2457–2490, 2021. doi: 10.1214/20-AOS2041.
- S. Brockhaus, D. Rügamer, and S. Greven. Boosting functional regression models with FDboost. *Journal of Statistical Software*, 94(10):1–50, 2020. doi: 10.18637/jss.v094.i10.
- A. Chakraborty and P. Chaudhuri. A wilcoxon–mann–whitney-type test for infinite-dimensional data. *Biometrika*, 102:239–246, 2015. doi: 10.1093/biomet/asu072.
- J. A. Cuesta-Albertos and M. Febrero-Bande. A simple multiway ANOVA for functional data. *Test*, 19:537–557, 2010. doi: 10.1007/s11749-010-0185-3.
- W. Dai and M. G. Genton. Multivariate functional data visualization and outlier detection. *Journal of Computational and Graphical Statistics*, 27:923–934, 2018. doi: 10.1080/10618600.2018.1473781.
- W. Dai, T. Mrkvička, Y. Sun, and M. G. Genton. Functional outlier detection and taxonomy by sequential transformations. *Computational Statistics & Data Analysis*, 149:106960, 2020. doi: <https://doi.org/10.1016/j.csda.2020.106960>.
- C.-Z. Di, D. M. Crainiceanu, B. S. Caffo, and N. M. Punjabi. Multilevel functional principal component analysis. *The Annals of Applied Statistics*, 3:458–488, 2009. doi: 10.1214/08-AOAS206.
- J. Gassen. Download Apple mobility trend reports data. *tidycovid19* https://joachim-gassen.github.io/tidycovid19/reference/download_apple_mtr_data.html, 2022. Accessed June, 2023.

- M. G. Genton, C. Johnson, K. Potter, G. Stenchikov, and Y. Sun. Surface boxplots. *Stat*, 3: 1–11, 2014. doi: <https://doi.org/10.1002/sta4.39>.
- J. Goldsmith, F. Scheipl, L. Huang, J. Wrobel, C. Di, J. Gellar, J. Harezlak, M. W. McLean, B. Swihart, L. Xiao, C. Crainiceanu, and P. T. Reiss. *refund: Regression with Functional Data*, 2022. URL <https://CRAN.R-project.org/package=refund>. R package version 0.1-28.
- S. Greven and F. Scheipl. A general framework for functional regression modelling. *Statistical Modelling*, 17:1–35, 2017. doi: 10.1177/1471082X16681317.
- P. Hall and I. Van Keilegom. Two sample tests in functional data analysis starting from discrete data. *Statistica Sinica*, 17:1511–1531, 2007. URL <https://www.jstor.org/stable/24307686>.
- M. Hollander and D. A. Wolfe. *Nonparametric statistical methods*. John Wiley & Sons, Inc., New York, 1999.
- H. Huang and Y. Sun. A decomposition of total variation depth for understanding functional outliers. *Technometrics*, 61:445–458, 2019. doi: 10.1080/00401706.2019.1574241.
- R. Katz, M. Boyce, and E. Graedon. Visualizing the impact of policies on COVID response. *COVID AMP* <https://covidamp.org/>, 2023. Accessed June, 2023.
- J. Kloeke and J. W. McKean. *Nonparametric Statistical Methods using R*. CRC Press, Taylor & Francis Group, Boca Raton, Florida, 2015.
- W. H. Kruskal and W. A. Wallis. Use of ranks in one-criterion variance analysis. *Journal of the American Statistical Association*, 47(260):583–621, 1952. doi: 10.2307/2280779.
- S. López-Pintado and J. Romo. On the concept of depth for functional data. *Journal of the American Statistical Association*, 104:718–734, 2009. doi: 10.1198/jasa.2009.0108.
- S. López-Pintado and J. Romo. A half-region depth for functional data. *Computational Statistics & Data Analysis*, 55:1679–1695, 2011. doi: 10.1016/j.csda.2010.10.024.
- S. López-Pintado and J. Wrobel. Robust non-parametric tests for imaging data based on data depth. *Stat*, 6:405–419, 2017. doi: 10.1002/sta4.168.
- S. López-Pintado, J. Romo, and A. Torrente. Robust depth-based tools for the analysis of gene expression data. *Biostatistics*, 11:254–264, 2010. doi: 10.1093/biostatistics/kxp056.
- H. B. Mann and D. R. Whitney. On a test of whether one of two random variables is stochastically larger than the other. *The Annals of Mathematical Statistics*, 18:50–60, 1947. doi: 10.1214/aoms/1177730491.
- R. Meléndez, R. Giraldo, and V. Leiva. Sign, Wilcoxon and Mann-Whitney tests for functional data: An approach based on random projections. *Mathematics*, 9:44, 2021. doi: 10.3390/math9010044.

- M. J. Meyer. Supplement A to “Doubly ranked tests for grouped functional data”. 2024a. doi: 10.1214/.
- M. J. Meyer. Supplement B to “Doubly ranked tests for grouped functional data”. 2024b. doi: 10.1214/.
- J. S. Morris. Functional regression. *Annual Review of Statistics and Its Application*, 2: 321–359, 2015. doi: 10.1146/annurev-statistics-010814-020413.
- G.-M. Pomann, A.-M. Staicu, and S. Ghosh. A two-sample distribution-free test for functional data with application to a diffusion tensor imaging study of multiple sclerosis. *Journal of the Royal Statistical Society, Series C*, 65:395–414, 2016. doi: 10.1111/rssc.12130.
- R Core Team. *R: A Language and Environment for Statistical Computing*. R Foundation for Statistical Computing, Vienna, Austria, 2022. URL <https://www.R-project.org/>.
- J. O. Ramsay and B. W. Silverman. *Functional Data Analysis*. Springer, New York, 2nd edition, 2005.
- J. O. Ramsay, G. Hooker, and S. Graves. *Functional Data Analysis in R and Matlab*. Springer, New York, 2009.
- J. O. Ramsay, S. Graves, and G. Hooker. *fda: Functional Data Analysis*, 2022. URL <https://CRAN.R-project.org/package=fda>. R package version 6.0.5.
- C. Sguera and S. López-Pintado. A notion of depth for sparse functional data. *Test*, 30: 630–649, 2021. doi: 10.1007/s11749-020-00734-y.
- Y. Sun and M. G. Genton. Functional boxplots. *Journal of Computational and Graphical Statistics*, 20:316–334, 2011. doi: 10.1198/jcgs.2011.09224.
- Y. Sun and M. G. Genton. Adjusted functional boxplots for spatio-temporal data visualization and outlier detection. *Environmetrics*, 23:54–64, 2012. doi: 10.1002/env.1136.
- Y. Sun, M. G. Genton, and D. W. Nychka. Exact fast computation of band depth for large functional datasets: How quickly can one million curves be ranked? *Stat*, 1:68–74, 2012. doi: <https://doi.org/10.1002/sta4.8>.
- J.-L. Wang, J.-M. Chiou, and H.-G. Müller. Functional data analysis. *Annual Review of Statistics and Its Application*, 3:257–295, 2016. doi: 10.1146/annurev-statistics-041715-033624.
- F. Wilcoxon. Individual comparisons by ranking methods. *Biometrics Bulletin*, 1:80–83, 1945. doi: 10.2307/3001968.
- J. Wrobel, S. Y. Park, A.-M. Staicu, and J. Goldsmith. Interactive graphics for functional data analyses. *Stat*, 5:108–118, 2016. doi: <https://doi.org/10.1002/sta4.109>.

- L. Xiao, Y. Li, and D. Ruppert. Fast bivariate p-splines: the sandwich smoother. *Journal of the Royal Statistical Society: Series B (Statistical Methodology)*, 75:577–599, 2013. doi: <https://doi.org/10.1111/rssb.12007>.
- L. Xiao, V. Zipunnikov, D. Ruppert, and C. Crainiceanu. Fast covariance estimation for high-dimensional functional data. *Statistics and Computing*, 26:409–421, 2016. doi: 10.1007/s11222-014-9485-x.
- F. Yao, H.-G. Müller, and J.-L. Wang. Functional linear regression analysis for longitudinal data. *Annals of Statistics*, 33:2873–2903, 2005. doi: 10.1214/009053605000000660.